Pramana – J. Phys. (2017) 89:60
DOI 10.1007/s12043-017-1454-4

Neutrino cross-section in ultrahigh energy regime using double asymptotic limit of QCD

KALPANA BORA[1,*], NEELAKSHI SARMA[1] and JAYDIP SINGH[2]

[1]Department of Physics, Gauhati University, Gopinath Bordoloi Nagar, Guwahati 781 014, India
[2]Department of Physics, Lucknow University, Lucknow 226 007, India
*Corresponding author. E-mail: kalpana.bora@gmail.com

Published online 5 October 2017

Abstract. Studies on neutrino–nucleon (νN) cross-sections have regained interest due to increasing importance of precision measurements, as they are needed as an ingredient in all neutrino experiments. In this work, we use the QCD-inspired double asymptotic limit fit of electron–proton structure function F_2^{ep} to low-x HERA data, to calculate νN cross-section for charged current (CC) and neutral current (NC) neutrino interactions in ultrahigh energy (UHE) neutrino energy (E_ν) regime (10^9 GeV $\leq E_\nu \leq 10^{12}$ GeV). The form $F_2^{ep} \sim x^{-\lambda(Q^2)}$, used in our analysis, can be conjectured like a dynamic pomeron (DP)-type behaviour. We also find an analytic form of the total cross-sections, $\sigma_{\rm CC}^{\nu N}$ and $\sigma_{\rm NC}^{\nu N}$, which appear to be of Reggeon exchange type. We also do a comparative analysis of our results with those available in literature. Future measurements will support/confront our predictions.

Keywords. Neutrino cross-section; ultrahigh energy; quantum chromodynamics; double asymptotic limit; dynamic pomeron; Reggeon.

PACS Nos 13.15.+g; 13.85.Lg; 12.40.Nn

1. Introduction

Neutrino–nucleon scattering cross-sections are used in all neutrino experiments, be it neutrinos coming from natural resources, or from artificial (man-made) resources [1]. In any neutrino experiment, neutrinos are scattered off a nucleon/nucleus of the detector. Number of events (of signal process) are observed experimentally, which is proportional to the flux of the incoming neutrinos, cross-section and probability of the signal process. Neutrinos coming to the Earth from natural sources have their origin in the Sun, active galactic nuclei (AGN) and core of supernovae – they are believed to play crucial roles in various astrophysical phenomena. The information obtained from astrophysical objects and mechanisms is complimentary to that available from electromagnetic or hadronic interactions. Neutrino interactions across different energy scales can be classified as [1]

(a) Thresholdless process ($E_\nu \sim$ 0–1 MeV)
These include coherent scattering and neutrino capture on radioactive nuclei (enhanced or stimulated beta decay emission).
(b) Low-energy nuclear process ($E_\nu \sim$ 0–100 MeV)
At such scale, target nucleus can be probed at the smallest length scales, ν is scattered off a nucleus.
(c) Intermediate energy process ($E_\nu \sim$ 0.1–20 GeV)
They can again be classified as charged current (also called quasielastic, QE) and neutral current (elastic) process. Neutrino scatters off an entire nucleon.
(d) High energy process ($E_\nu \sim$ 20–500 GeV)
Neutrino can resolve individual quark constituents of the nucleon, also called as deep inelastic scattering (DIS) process.
(e) Ultrahigh energy (UHE) process ($E_\nu \sim$ 0.5 TeV–1 EeV)
The latest highest energy neutrino recorded so far is ∼PeV [2] and this has opened avenue for researchers to work with UHE neutrinos from astrophysical resources [3].

Neutrino DIS processes have been used to validate the Standard Model (SM) and also to probe nucleon structure. Cross-sections, electroweak (EW) parameters, coupling constants, scaling variables etc. have also been measured by experimentalists through such processes. In the νN DIS, the neutrino scatters off a quark in the nucleon via the exchange of a virtual W (CC)

or Z (NC) boson, producing a lepton and hadronic system in the final state. Similarly, UHE neutrino cross-sections have gained importance as many experiments worldwide are ongoing/planned to observe processes involving them. The natural sources of UHE could be supernovae core collapse, cosmic rays, γ-ray burst, AGN etc. and they serve as windows for understanding highest energy processes in the Universe. As attenuation of these neutrinos due to their travel is very low (as they are only weakly interacting), they act as powerful tools to help us know about their sources. The ongoing and planned experiments for measuring UHE neutrinos are: Baikal [4], ANITA [5], RICE [6], AMANDA [7], HiRes [8], ANTARES [9] , IceCube [10], GLUE [10,11], Pierre Auger Cosmic Ray Observatory [12], ARIANNA [13], JEM-EUSO [14]. A number of studies on UHE neutrino cross-sections (CC and NC) are available in literature. Gandhi *et al* [3] (GQRS 1998) reported results based on u, d, c, s quark PDFs (parton distribution function) from 1998 CTEQ4 analysis of the early HERA-ZEUS small-x data. In the results presented by Connolly *et al* [15] (CTW 2011) and Cooper-Sarkar *et al* [16] (CSMS 2011) they included b-quark contribution to both CC and NC scattering and are based on updated PDFs obtained from newer data. Froissart bound inspired behaviour of F_2^{ep} of DIS (e–p) scattering was used by Martin M Block *et al* [17] (BDHM 2013) to evaluate UHE neutrino cross-section off an isoscalar nucleon $N = (n + p)/2$, upto $E_\nu \sim 10^{17}$ GeV. It may be noted that $E_\nu \sim 10^{17}$ GeV is the highest reach of the experimental search for UHE cosmic neutrino [10,11]. In this work, we calculate CC and NC neutrino–nucleon scattering cross-section with $E_\nu \sim (10^9$–10^{12} GeV) using QCD-inspired double asymptotic limit (DAL) of the structure function $F_2^{ep}(x, Q^2)$. The preliminary results of this analysis were presented in [18] of (e–p) DIS [19]. In [19], one of us found that a form

$$F_2^{ep} \sim x^{-\lambda(Q^2)}, \tag{1}$$

can be derived from DGLAP evolution equation [18], which was found to describe the available HERA H1 data [19] for F_2^{ep} in the range $1 \leq x \leq 10^{-4}$ and $5 \leq Q^2 \leq 5000$ GeV^2 within 10% error. It is worth mentioning that this behaviour (eq. (1)) of F_2^{ep} can be viewed as of dynamic-pomeron type. In physics the pomeron is a Regge trajectory, a family of particles with increasing spin, postulated to explain the slowly rising cross-section of hadronic collisions at high energies. At high energies (and low Q^2) $\gamma^* p$ cross-section is believed to be similar to the cross-section of hadron–hadron interactions. Pomeron-type behaviour of F_2 at small x can explain the logarithmic rise of cross-section with energy. In figure 1 we present the result from

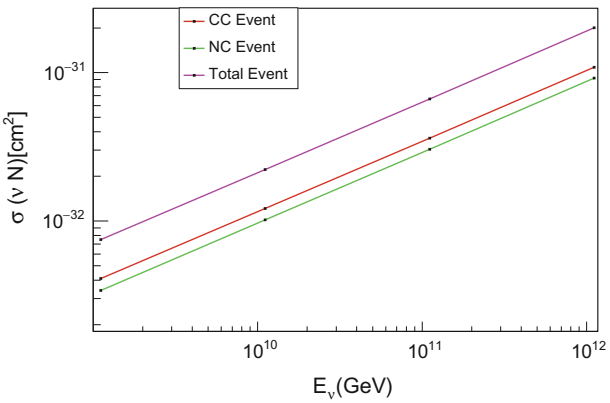

Figure 1. Variation of neutrino–nucleon charged current, neutral current and total current cross-sections with neutrino energy (from our calculation).

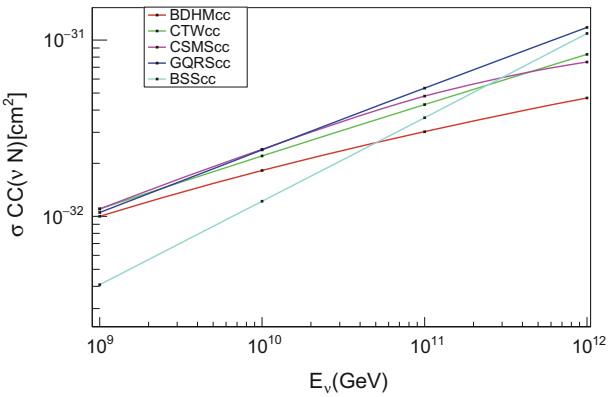

Figure 2. Comparison of charged current νN cross-sections in cm^2 as a function of E_ν.

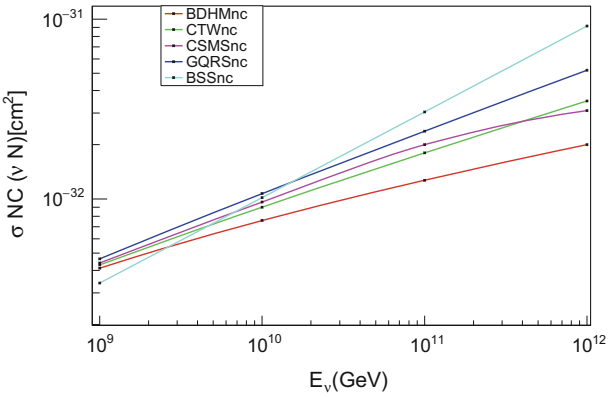

Figure 3. Comparison of neutral current νN cross-sections in cm^2 as a function of E_ν.

the computation for CC, NC and total cross-section for $10^9 \leq E_\nu \leq 10^{12}$ GeV. We then compare our results (shown in figures 2 and 3) in the energy range $10^9 \leq E_\nu \leq 10^{12}$ GeV with those already available in literature. While the overall behaviour is found to

be similar, the values of our cross-sections are found to be lower than those of BDHM2013, CTW2011 and CSMS2011 for $E_\nu \geq (10^9$–$10^{11})$ GeV for CC. On the other hand, our value of cross-section is slightly lower than GQRS1998, for $E_\nu = 10^9$ GeV. For NC, for $E_\nu \geq (10^9$–$10^{12})$ GeV, our values are almost the same as GQRS1998 whereas for $E_\nu \geq (10^9$–$10^{10})$ GeV our values are slightly lower than BDHM2013, CTW2011 and CSMS2011. Then we present the analytical form of total cross-section, fitted to a form, both for CC and NC. The behaviour of eqs (19) and (20) appears like a Reggeon exchange type.

It has been stated in [1] that for a more accurate prediction of the νN cross-section, a well-formulated model of the nucleon structure function is needed and that this predictive power is specially important in the search of new physics (NP). At such ultrahigh energies, the νN cross-section can depart substantially from the Standard Model predictions, if NP is at play. Study of such UHE neutrino interaction thus can be a possible probe of new physics. Determination/measurement of νN cross-section can also be useful to constrain the underlying QCD dynamics of the nucleon. Detection of UHE neutrino events may shed light on the observation of air shower events with energies $\geq 10^{10}$ GeV, as well. Moreover, the behaviour of UHE νN cross-section can also be used to discriminate among different models of gluon dynamics at play at very low x. The energy dependence of total νN cross-section measurement may have important implications for hadronic interactions at such UHE, not accessible otherwise. If cross-section much outside the limits of ongoing/planned neutrino experiments are observed, then predictions presented in this work can be very important. This commands attention also, as many experiments worldwide are planned/ongoing in DIS/UHE regime.

The paper has been organized as follows. In §2 we present a review on DAL behaviour of F_2^{ep}, following ref. [19]. In §3, analytical formulae for $\sigma_{\nu N}^{\rm CC}$ and $\sigma_{\nu N}^{\rm NC}$ using the above form of F_2^{ep} are presented. Numerical calculations, results and analysis are shown in §4. Summary and conclusions are presented in §5.

2. $F_2^{ep}(x, Q^2)$ in DAL of QCD: A brief review

In this section, we give a brief review of the behaviour of $F_2^{ep}(x, Q^2)$ using DAL of QCD, following [19], for the sake of completeness of this work. In DIS (e–p) scattering, the incoming electron scatters off the target proton, via the exchange of a virtual photon, producing a hadronic system in the final state. A typical (e–p) DIS event can be described with the help of two independent variables, x and Q^2, where x is the Bjorken variable (fraction of protons momentum carried by its constituent partons, in Breit's frame) and Q^2 is the transverse momentum squared of the virtual exchanged photon. The scattering cross-section can be described in terms of the two structure functions, $F_2(x, Q^2)$ and $F_1(x, Q^2)$. Bjorken variable $x = Q^2/2M\nu$, where ν is the energy loss of the electron and Q^2 depends on the scattering angle. The squared mass W^2 of the observed hadronic system is

$$W^2 = (p+q)^2 = M^2 - Q^2 + 2M\nu, \tag{2}$$

(in proton's rest frame) where p and q are momenta of the proton and the electron respectively, M is the mass of the proton. For elastic scattering, $W^2 = M^2(x = 1)$. In parton model, at large Q^2, for spin $\frac{1}{2}$ partons, $F_2(x) = 2xF_1$ and $F_L = F_2 - 2xF_1 = 0$.

For point-like parton, Bjorken scaling occurs, structure function do not depend on Q^2. But scaling violations are found to occur in (e–p) DIS processes, as x decreases, which means that structure function F_2^{ep} depends on Q^2 also. Thus, the proton no longer consists of point-like partons only, but has a dynamic structure deep inside, which can be explained via QCD evolution equations in leading log Q^2 approximation (LLQ^2), known as DGLAP equations. In (e–p) DIS, in the next to leading order, scaling violations occur through gluon bremsstrahlung from quarks and quark pair creation from gluons. At small $x < 10^{-2}$, the latter process dominates the scaling violations. This property can be exploited to extract gluon density from the slope $\mathrm{d}F_2/\mathrm{d}\ln Q^2$ of the proton structure function. The general equations [14] describing the Q^2 evolution of the quark density and gluon density respectively are

$$\frac{\mathrm{d}q^i(x,t)}{\mathrm{d}t} = \frac{\alpha(t)}{2\pi}\int_x^1 \frac{\mathrm{d}y}{y}\left[\sum_{j=1}^{2f} q^j(y,t)P_{qq}\left(\frac{x}{y}\right) + G(y,t)P_{qg}\left(\frac{x}{y}\right)\right], \tag{3}$$

$$\frac{\mathrm{d}G(x,t)}{\mathrm{d}t} = \frac{\alpha(t)}{2\pi}\int_x^1 \frac{\mathrm{d}y}{y}\left[\sum_{j=1}^{2f} q^j(y,t)P_{gq}\left(\frac{x}{y}\right) + G(y,t)P_{gg}\left(\frac{x}{y}\right)\right], \tag{4}$$

where $P_{qq}(x/y)$, $P_{qg}(x/y)$, $P_{gq}(x/y)$, $P_{gg}(x/y)$ are the splitting functions and $t = \ln(Q^2/Q_0^2)$. Assuming that the quark densities are negligible and the non-singlet contribution $F_2^{\rm NS}$ can be ignored safely at small x in DGLAP equation, for F_2, the equation becomes

$$\frac{\mathrm{d}F_2(x,Q^2)}{\mathrm{d}\ln Q^2} = \frac{10\alpha_s}{9\pi}\int_x^1 \mathrm{d}x' P_{qg}(x')\frac{x}{x'}g\left(\frac{x}{x'},Q^2\right). \tag{5}$$

Here $xg(x,Q^2) = G(x,Q^2)$ is the gluon momentum density and $g(x,Q^2)$ is the gluon number density of the proton and $x/x' = x/y$. Rearranging eq. (5) we have

$$\frac{\mathrm{d}F_2(x,Q^2)}{\mathrm{d}\ln Q^2} = \frac{5\alpha_s}{9\pi}\int_x^1 \mathrm{d}y\frac{x}{y}g(y,Q^2) \times \frac{1}{y^2}[x^2+(y-x)^2]. \tag{6}$$

Substituting $y = x/(1-z)$ we can write RHS of eq. (6) as

$$\frac{5\alpha_s}{9\pi}\int_0^{1-x}\mathrm{d}z G\left(\frac{x}{1-z},Q^2\right)[z^2+(1-z)^2]. \tag{7}$$

Expanding $G(x/(1-z),Q^2)$ about $z=(1-x)/2$ and keeping terms upto the first derivative of G in the expansion we have

$$G\left(\frac{x}{1-z},Q^2\right) = G\left(\frac{2x}{1+x},Q^2\right) + \left(z-\frac{1-x}{2}\right)\frac{4x}{(1+x)^2}\frac{\mathrm{d}G(x'',Q^2)}{\mathrm{d}x''}\bigg|_{x''=\frac{2x}{1+x}}. \tag{8}$$

When this expansion is used in eq. (6) we get

$$\frac{\mathrm{d}F_2(x,Q^2)}{\mathrm{d}\ln Q^2} = \frac{5\alpha}{9\pi}\frac{(A+Ax+2B)^2}{(1+x)(A+Ax+4B)}G(y',Q^2), \tag{9}$$

where

$$y' = \left[\frac{2x}{1+x}\frac{(A+Ax+4B)}{(A+Ax+2B)}\right],$$

$$A = \left[\frac{2(1-x)^3}{3} - (1-x)^2 + (1-x)\right],$$

and

$$B = \left[\frac{(1-x)^4-(1-x)^3}{6}\right].$$

In the limit $x \to 0$, eq. (9) reduces to

$$\frac{\mathrm{d}F_2(x,Q^2)}{\mathrm{d}\ln Q^2} = \frac{10\alpha_s}{9\pi}\frac{(1-x)^2}{(1-1.5x)}G\left(2x\frac{(1-1.5x)}{(1-x^2)},Q^2\right). \tag{10}$$

Using the above, double asymptotic expression [19] for F_2 in small x and large Q^2 (DAL) limit, we can write

$$F_2^p \sim \frac{\exp\sqrt{\frac{144}{33-2n_f}\xi\ln\left(\frac{1}{x_1}\right)}}{\left(\frac{144}{33-2n_f}\xi\ln\left(\frac{1}{x_1}\right)\right)^{1/4}}, \tag{11}$$

with

$$\xi = \ln\left(\frac{\ln(Q^2/\Lambda^2)}{\ln(Q_0^2/\Lambda^2)}\right), \quad x_1 = \frac{2x-3x^2}{1-x^2},$$

n_f is the number of flavours, Q_0^2 is the value at which the input parton parametrization is to be used and Λ is the QCD mass scale. F_2^p in eq. (11) in DAL can be parametrized as

$$F_2^p \sim x^{-\lambda(Q^2)}, \tag{12}$$

which can be viewed as of dynamic pomeron-type.

3. $\sigma_{\nu N}^{\mathrm{CC}}$ and $\sigma_{\nu N}^{\mathrm{NC}}$ in DAL of QCD

The total charged and neutral current (CC and NC) for neutrino–nucleon scattering [17], for an isoscalar nucleon $N = (n+p)/2$, can be written as

$$\sigma_{\mathrm{CC}}^{\nu N}(E_\nu) = \int_{Q^2_{\min}}^{s}\mathrm{d}Q^2\int_{Q^2/s}^1\mathrm{d}x\frac{\mathrm{d}^2\sigma_{\mathrm{CC}}}{\mathrm{d}x\mathrm{d}Q^2}(E_\nu,Q^2,x)$$
$$= \frac{G_{\mathrm{F}}^2}{4\pi}\int_{Q^2_{\min}=1}^{2mE_\nu}\mathrm{d}Q^2\left(\frac{M_W^2}{Q^2+M_W^2}\right)^2 \times \int_{Q^2/2mE_\nu}^1\frac{\mathrm{d}x}{x}\Big[F_2^\nu + xF_3^\nu + (F_2^\nu - xF_3^\nu) \times \left(1-\frac{Q^2}{xs}\right)^2 - \left(\frac{Q^2}{xs}\right)^2 F_L^\nu\Big], \tag{13}$$

where F_2^ν is the neutrino–nucleon structure function, $s = 2mE_\nu$ where s is the Mandelstam variable which is the total energy in the centre of mass frame, m is the nucleon mass, G_{F} is the Fermi constant, M_W^2 is the squared mass of the intermediate W-boson and Q^2 is the four-momentum square of virtual photon. Here, xF_3 is a measure of difference of quarks and antiquarks PDFs, and so is sensitive to the valence quark distribution function. We neglect valence quark contribution in our analysis, as at small x, structure of proton is dominated by gluons only [19]. Therefore, contributions of F_3^ν to νN scattering is subdominant only and hence neglected in our analysis. Similar expression can be obtained for neutral current cross-section by replacing M_W by M_Z in eq. (13). For the flavour-symmetric $(q\bar{q})N$ interaction at small $x < 0.1$, the neutrino–nucleon structure function, $F_2^\nu(x,Q^2)$, can be related to electromagnetic structure function, $F_2^{ep}(x,Q^2)$ [20] as

$$F_2^{\nu}(x, Q^2) = \frac{n_f}{\sum_q^{n_f} Q_q^2} F_2^p(x, Q^2), \tag{14}$$

where n_f is the number of flavours and Q_q is the charge of the quark. Thus, for $10^9 < E_\nu < 10^{12}$, x lies in the range $10^{-5} < x < 10^{-8}$. Here $\sigma^{\nu N}_{\mathrm{CC,NC}}$ is the neutrino–nucleon cross-section to leading order in weak coupling G_F and all orders in strong hadronic interaction.

Minimum value of Q^2 is consistent with the application of pQCD. We have used $Q^2_{\min} = 1$ GeV^2 in our computation. Now using DAL value of F_2^{ep} from eq. (12) in eq. (13), we obtain the expression for total neutrino–nucleon cross-sections as

$$\sigma^{\nu N}_{\mathrm{CC}}(E_\nu) \approx \frac{G_\mathrm{F}^2}{4\pi} \int_{Q^2_{\min}=1}^{2mE_\nu \times 10^{-2}} \mathrm{d}Q^2 \left(\frac{M_W^2}{Q^2 + M_W^2}\right)^2 \times \int_{Q^2/2mE_\nu}^{1} \frac{\mathrm{d}x}{x}(x^{-\lambda(Q^2)}), \tag{15}$$

where $\lambda(Q^2) = a - be^{-cQ^2}$ and the values of constants are found to be: $a = 0.486$, $b = 0.272$ and $c = 0.002$. Solving eq. (15) we get

$$\sigma^{\nu N}_{\mathrm{CC}}(E_\nu) = A\frac{G_\mathrm{F}^2}{4\pi} \int_{Q^2_{\min}=1}^{2mE_\nu \times 10^{-2}} \frac{\mathrm{d}Q^2}{-\lambda(Q^2)} \left(\frac{M_W^2}{Q^2 + M_W^2}\right)^2 \times x^{-\lambda(Q^2)}\Big|_{Q^2/2mE_\nu}^{1}$$

$$= -A\frac{G_\mathrm{F}^2}{4\pi} \int_{Q^2_{\min}=1}^{2mE_\nu \times 10^{-2}} \frac{\mathrm{d}Q^2}{\lambda(Q^2)} \left(\frac{M_W^2}{Q^2 + M_W^2}\right)^2 \times \left\{1 - \left(\frac{Q^2}{2mE_\nu}\right)^{-\lambda(Q^2)}\right\}, \tag{16}$$

$$= A\frac{G_\mathrm{F}^2 M_W^4}{4\pi} \int_{Q^2_{\min}=1}^{2mE_\nu \times 10^{-2}} \frac{\mathrm{d}Q^2}{\lambda(Q^2)} \left(\frac{1}{Q^2 + M_W^2}\right)^2 \times \left\{\left(\frac{Q^2}{2mE_\nu}\right)^{-\lambda(Q^2)} - 1\right\}, \tag{17}$$

in low-x and high-Q^2 regime. Here A is the normalization constant.

The corresponding total neutral current cross-section $\sigma^{\nu N}_{\mathrm{NC}}(E_\nu)$ is obtained by replacing M_W by squared mass of intermediate Z boson M_Z, that is

$$\sigma^{\nu N}_{\mathrm{NC}}(E_\nu) = A\frac{G_\mathrm{F}^2 M_Z^4}{4\pi} \int_{Q^2_{\min}=1}^{2mE_\nu \times 10^{-2}} \frac{\mathrm{d}Q^2}{\lambda(Q^2)} \left(\frac{1}{Q^2 + M_Z^2}\right)^2 \times \left\{\left(\frac{Q^2}{2mE_\nu}\right)^{-\lambda(Q^2)} - 1\right\}. \tag{18}$$

4. Results and discussion

We have computed $\sigma^{\nu N}_{\mathrm{CC}}$ and $\sigma^{\nu N}_{\mathrm{NC}}$ and have presented the results in figure 1. We find that the behaviour of $\sigma^{\nu N}_{\mathrm{CC}}$ and $\sigma^{\nu N}_{\mathrm{NC}}$ is similar to that available in literature. Tables 1 and 2 show a comparison of our results with those of earlier works. We then make a fit to the CC and

Table 1. Charged current νN cross-sections, in cm^2 as a function of E_ν are listed.

E_ν (GeV)	σ_{BDHM} (cm^2)	σ_{CTW} (cm^2)	σ_{CSMS} (cm^2)	σ_{GQRS} (cm^2)	σ_{BSS} (cm^2)
10^9	1.00×10^{-32}	1.1×10^{-32}	1.1×10^{-32}	1.05×10^{-32}	4.09×10^{-33}
10^{10}	1.82×10^{-32}	2.2×10^{-32}	2.4×10^{-32}	2.38×10^{-32}	1.21×10^{-32}
10^{11}	3.02×10^{-32}	4.3×10^{-32}	4.8×10^{-32}	5.34×10^{-32}	3.62×10^{-32}
10^{12}	4.69×10^{-32}	8.3×10^{-32}	7.5×10^{-32}	1.18×10^{-31}	1.08×10^{-31}

Here BDHM refers to the work done by Martin M Block *et al* [17], CTW refers to Connolly *et al* [15], CSMS refers to Cooper-Sarkar *et al* [16], GQRS refers to Gandhi *et al* [3] and BSS refers our work in this paper.

Table 2. Neutral current νN cross-sections, in cm^2 as a function of E_ν are listed.

E_ν (GeV)	σ_{BDHM} (cm^2)	σ_{CTW} (cm^2)	σ_{CSMS} (cm^2)	σ_{GQRS} (cm^2)	σ_{BSS} (cm^2)
10^9	4.12×10^{-33}	4.3×10^{-33}	4.4×10^{-33}	4.64×10^{-33}	3.40×10^{-33}
10^{10}	7.58×10^{-33}	9.0×10^{-33}	9.6×10^{-33}	1.07×10^{-32}	1.016×10^{-32}
10^{11}	1.27×10^{-32}	1.8×10^{-32}	2.0×10^{-32}	2.38×10^{-32}	3.042×10^{-32}
10^{12}	2.00×10^{-32}	3.5×10^{-32}	3.1×10^{-32}	5.20×10^{-32}	9.16×10^{-32}

Here BDHM refers to the work done by Martin M Block *et al* [17], CTW refers to Connolly *et al* [15], CSMS refers to Cooper-Sarkar *et al* [16], GQRS refers to Gandhi *et al* [3] and BSS refers our work in this paper.

NC ν–N cross-sections to obtain the analytic forms of the following types in the energy range 10^9 GeV $\leq E_\nu \leq 10^{12}$ GeV:

$$\sigma_{\nu N}^{\mathrm{CC}} = (2.009 \pm 0.011)(\ln E_\nu)^2 + (-4.457 \pm 0.035) \times (\ln E_\nu) + (-32.299 \pm 0.062), \quad (19)$$

$$\sigma_{\nu N}^{\mathrm{NC}} = (2.015 \pm 0.010)(\ln E_\nu)^2 + (-4.467 \pm 0.038) \times (\ln E_\nu) + (-32.387 \pm 0.057). \quad (20)$$

This can be viewed as a Reggeon exchange-type behaviour of the cross-section at UHE.

Here, we would like to emphasize that, a dynamic pomeron-type form of F_2^{ep} (eq. (1)), of the strong interactions, gives a Reggeon exchange-type behaviour of (eqs (19) and (20)) total cross-section of weak interactions. This can point out to some interplay between strong and weak interactions.

5. Summary

To summarize, in this work we calculated total neutrino–nucleon cross-section $\sigma_{\nu N}^{\mathrm{CC}}$ for CC and $\sigma_{\nu N}^{\mathrm{NC}}$ for NC interactions using the double asymptotic limit of F_2^{ep} of DIS $(e - p)$ scattering, found earlier by one of us [19]. In refs [3,15–17], they used standard sets of parton distribution functions available in literature at that times, to obtain total cross-sections at UHE, but we have used our own parametrization for F_2^{ep} (within 10% error) in DAL, using input PDFs at Q^2_{min}. We found that though the overall behaviour of our calculated νN cross-sections is similar to the above-mentioned works, our values are slightly smaller, in the low-energy range, while larger in the high-energy range. This difference could be attributed to different assumptions in input parameterization of PDFs used in F_2^{ep}, and due to the fact that we have used our own analytic form of F_2^{ep} in low-x and large-Q^2 regime obtained from DGLAP equation: We note that with the use of screening corrections in the evolution of proton structure function, these results can be improved, and will be done in future works. We used Monte Carlo integration technique in our computation to obtain these cross-sections in the energy range 10^9 GeV $\leq E_\nu \leq 10^{12}$ GeV. Then we did a parameter fitting of these cross-sections, to obtain their analytical form (eqs (19) and (20)). The dynamical pomeron-type behaviour of F_2^{ep} give rise to a Reggeon exchange-type behaviour of total cross-section in UHE regime. This could hint to some interplay between strong (F_2^{ep}) and weak ($\sigma^{\nu N}$) dynamics. The future measurements of $\sigma^{\nu N}$ in this regime would provide a test to the ideas presented in the work.

Acknowledgements

K Bora and N Sarma would like to thank DST-SERB, Govt. of India, for a project; Grant No. DST-SERB/EMR/2014/000296 under which this work is done. N Sarma also thanks Prof. Raj Gandhi, for financial support and useful discussions at Harish Chandra Research Institute (HRI), Allahabad, India, where a part of this work has been done. J Singh is grateful to HRI, Allahabad.

References

[1] J A Formaggio and G P Zeller, *Rev. Mod. Phys.* **84**, 1307 (2012)
[2] IceCube Collaboration: M G Aartsen *et al*, *Phys. Rev. Lett.* **111**, 021103 (2013), arXiv:1304.5356
[3] R Gandhi *et al*, *Phys. Rev. D* **58**, 093009 (1998), arXiv:hep-ph/9807264
[4] A D Avrorin *et al*, *Astropart. Phys.* **62**, 12 (2015), arXiv:1405.3551
[5] ANITA Collaboration: S Hoover *et al*, *J. Phys.: Conf. Ser.* **81**, 012009 (2007)
[6] RICE Collaboration: I Kravchenko *et al*, *Phys. Rev. D* **85**, 062004 (2012)
[7] AMANDA Collaboration: J Ahrens *et al*, *Nucl. Instrum. Methods A* **524**, 169 (2004)
[8] HiRes Collaboration: R Abbasi *et al*, *Ap. J.* **684**, 790 (2008)
[9] ANTARES Collaboration: A Gleixner *et al*, *EPJ Web of Conferences* **70**, 00070 (2014)
[10] IceCube Collaboration: M Aartsen *et al*, arXiv:1405.5303 (2014)
[11] GLUE Collaboration: P Gorham *et al*, *Phys. Rev. Lett.* **93**, 041101 (2004)
[12] Pierre Auger Collaboration: A Aab *et al*, *Phys. Rev. D* **93**, 072006 (2016)
[13] ARIANNA Collaboration: Stuart A Kleinfelder, presented at the 2015 IEEE Nuclear Science Symposium, arXiv:1511.07525
[14] JEM-EUSO Collaboration: Andreas Haungs *et al*, *J. Phys.: Conf. Ser.* **632**, 012092, arXiv:1504.02593.
[15] A Connolly *et al*, *Phys. Rev. D* **83**, 113009 (2011), arXiv:1102.0691
[16] A Cooper-Sarkar *et al*, *J. High Energy Phys.* **08**, 042 (2011), arXiv:1106.3723
[17] Martin M Block *et al*, *Phys. Rev. D* **88**, 013003 (2013), arXiv:1302.6127
[18] Kalpana Bora and Neelakshi Sarma, *Springer Conference Proceedings* **174**, 345 (2015), arXiv:1511.02676
[19] Kalpana Bora, *Polarised and unpolarised structure functions of nucleons at low-x*, Ph.D. Thesis (Gauhati University, 1998)
[20] M Kuroda and D Schildknecht, *Phys. Rev. D* **88**, 053007 (2013)